Results of the CCRI(II)-S12.H-3 supplementary comparison: Comparison of methods for the calculation of the activity and standard uncertainty of a tritiated-water source measured using the LSC-TDCR method

Philippe Cassette, Timotheos Altzitzoglou, Andrei Antohe, Mario Rossi, Arzu Arinc, Marco Capogni, Raphael Galea, Arunas Gudelis, Karsten Kossert, K.B. Lee, et al.

Results of the CCRI(II)-S12.H-3 supplementary comparison: Comparison of methods for the calculation of the activity and standard uncertainty of a tritiated-water source measured using the LSC-TDCR method

Philippe Cassette[1], Timotheos Altzitzoglou[2], Andrei Antohe[3], Mario Rossi[4], Arzu Arinc[5], Marco Capogni[6], Pierino de Felice[6], Raphael Galea[7], Arunas Gudelis[8], Karsten Kossert[9], K.B. Lee[10], Juncheng Liang[11], Youcef Nedjadi[12], Pilar Oropesa Verdecia[13], Tanya Shilnikova[14], Winifred van Wyngaardt[15], Tomasz Ziemek[16], Brian Zimmerman[17]

[1] *CEA LIST Laboratoire National Henri Becquerel (LNE-LNHB), CEA-Saclay, 91191 Gif sur Yvette Cedex, France*
[2] *European Commission, Joint Research Centre, (JRC), Directorate for Nuclear Safety and Security, Retieseweg 111, B-2440 Geel, Belgium*
[3] *Horia Hulubei National Institute for R&D in Physics and Nuclear Engineering (IFIN-HH), Magurele, RO 0-77125, Romania*
[4] *Laboratorio de Metrología de Radioisótopos (CNEA), Av. Del Libertador 8250 – CABA, Argentina*
[5] *National Physical Laboratory (NPL), Teddington, Middlesex TW11 0LW, UK*
[6] *National Institute of Ionizing Radiation Metrology,(ENEA- INMRI), Centro Ricerche Casaccia, Via Anguillarese, 301 - S.M. Galeria I-00123 Roma, Italy*
[7] *National Research Council of Canada (NRC), 1200 Montreal Road, Ottawa, ON, Canada K1A0R6*
[8] *Ionizing Radiation Metrology Laboratory, Center for Physical Sciences and Technology (FTMC), Savanoriu Ave. 231, LT-02300 Vilnius, Lithuania*
[9] *Physikalisch-Technische Bundesanstalt (PTB), Bundesallee 100, 38116 Braunschweig, Germany*
[10] *Korea Research Institute of Standards and Science (KRISS), Yuseong, Daejeon 305-340, Republic of Korea*
[11] *Division of Ionizing Radiation Metrology, National Institute of Metrology (NIM), Beijing 100029, China*
[12] *Institut de Radiophysique (IRA-METAS), CHUV, Rue du Grand-Pré 1, CH-1007 Lausanne, Switzerland*
[13] *Centro de Isótopos (CENTIS). Guanabacoa, La Habana 11100, Cuba*
[14] *D.I. Mendeleyev Institute for Metrology (VNIIM), 190005 Moskovsky pr., 19, St. Petersburg, Russia*
[15] *Australian Nuclear Science and Technology Organisation (ANSTO), New Illawarra Road, Lucas Heights NSW 2234, Australia*
[16] *National Centre for Nuclear Research Radioisotope Centre POLATOM (NCBJ RC POLATOM), Andrzeja Sołtana 7, 05-400 Otwock, Poland*
[17] *Physical Measurement Laboratory, National Institute of Standards and Technology (NIST), Gaithersburg, MD USA*

Abstract

A comparison of calculations of the activity of a $^{3}H_2O$ liquid scintillation source using the same experimental data set collected at the LNE-LNHB with a triple-to-double coincidence ratio (TDCR) counter was completed. A total of 17 laboratories calculated the activity and standard uncertainty of the LS source, using the files with experimental data. The results, as well as relevant information on the computation techniques are presented and analysed in this paper. All results are compatible, even if there is a significant dispersion between the reported

uncertainties. An output of this comparison is the estimation of the dispersion of TDCR measurement results when measurement conditions are well defined.

1 Introduction

The purpose of this exercise was to compare the calculation methods used at the National Metrology Institutes (NMIs) or Designated Institutes (DIs) to determine the value and the standard uncertainty of the activity of a ^3H_2O liquid scintillation counting (LSC) source, using the same experimental data set collected at the LNE-LNHB with a triple-to-double coincidence ratio (TDCR) counter and, to analyse potential reasons for the observed differences. The detection efficiency has been varied using two different methods: by adding coaxial grey filters around the source and by defocusing the photomultiplier tubes (PMT). The measurement results were presented in raw acquisition files and summarized in a spreadsheet. Even if all laboratories analysed the same data set, some variability in the activity results was expected, as the calculation of the detection efficiency can be made using various models, nuclear data, procedures or algorithms.

2 Participants

Seventeen laboratories participated in the calculation comparison piloted by LNE-LNHB. The participating laboratories and contact persons are presented in Table 1.

Table 1 List of participants

NMI/DI	Country	Responsible person	E-mail
ANSTO	Australia	Winifred van Wyngaardt	freda@ansto.gov.au
CENTIS	Cuba	Pilar Oropesa Verdecia	poropesa@centis.edu.cu
CNEA	Argentina	Mario Rossi	mprossi@cae.cnea.gov.ar
ENEA-INMRI	Italy	Marco Capogni	marco.capogni@enea.it
FTMC	Lithuania	Arunas Gudelis	arunas.gudelis@ftmc.lt
IFIN-HH	Romania	Andrei Antohe	antohe@nipne.ro
IRA-METAS	Switzerland	Youcef Nedjadi	youcef.nedjadi@chuv.ch
EC-JRC	EC	Timotheos Altzitzoglou	timotheos.altzitzoglou@ec.europa.eu
KRISS	Korea	K.B. Lee	lee@kriss.re.kr
LNE-LNHB	France	Philippe Cassette	philippe.cassette@cea.fr
NIM	China	Juncheng Liang	liangjc@nim.ac.cn
NIST	USA	Brian Zimmerman	bez@nist.gov
NPL	UK	Arzu Arinc	arzu.arinc@npl.co.uk
NRC	Canada	Raphael Galea	raphael.galea@nrc-cnrc.gc.ca
POLATOM	Poland	Tomasz Ziemek	tomasz.ziemek@polatom.pl
PTB	Germany	Karsten Kossert	karsten.kossert@ptb.de
VNIIM	Russia	Tanya Shilnikova	shti@vniim.ru

3 Protocol and experimental data sets

The experimental data provided for this comparison were obtained with an LSC TDCR counter. The measurand to be determined was the activity of the source at the measurement date with its standard uncertainty. The measurement conditions are described hereafter.

3.1 Source:

A volume of 15 ml of Ultima Gold® scintillator1 was poured into a 20 ml diffusive glass vial (Perkin Elmer® "high performance glass vial"). The outer face of the glass vial was sandblasted to get a rough and optically diffusive surface. The amount of tritiated water was about 40 mg and no chemical was added to stabilize the source. As the measurand was the activity of the source, no uncertainty component due to weighing was to be considered.

3.2 TDCR counter:

The source and a blank were measured using the TDCR1 counter of LNHB. The PMT are BURLE 8850 models, with diffusive entrance windows. The efficiencies of the tubes are not equal and it was mentioned in the protocol that this asymmetry had to be considered in the calculation of the detection efficiency, or an uncertainty term related to this asymmetry had to be taken into account. The relative experimental quantum efficiencies of the photocathodes of the tubes are 0.3079, 0.3799 and 0.3122 for tubes A, B and C, respectively. This information was not mentioned in the protocol but could be deduced from the full analysis involving solving a system of equations for the triples-to-doubles coincidence ratios as functions of the three individual double coincidence counting rates (AB, BC, AC).

The nominal voltages used are 2500 V for the anode, 800 V for the first dynode and from 700 V to 800 V for the focusing electrode, and the photocathode was at ground potential. The 700 V focusing voltage is the minimum allowed for this counter, a lower value inducing an excessive noise in the single PMT counting rates.

Acquisition electronics were composed of fast preamplifiers, constant fraction discriminators (CFD) and the MAC3 [1] module. The CFD thresholds were adjusted in the valley before the single photoelectron peak. The coincidence resolving time was 40 ns and the base duration of the dead-time, common to the three channels, was 50 µs. This dead-time was extendible. The live time was calculated using the live-time clock integrated within the MAC3 module. The reference oscillator is derived from the 10 MHz signal of a rubidium oscillator with a relative uncertainty lower than 10^{-10}.

Coincidence signals, as well as non-coincidence signals, were recorded. In order to simplify the resulting data, single PMT counting rates were not given in the Excel file but could be found, if needed, in the raw acquisitions files. It was pointed out that there is a huge fluctuation with time of the individual PMT counting rates, due to the evolution of the thermal noise of the photocathodes. The dead-time was also presented in the raw acquisitions files, in order to give the possibility to calculate the probability of accidental coincidences and the uncertainty of the live-time clock. The reference oscillator used in

1 Where any commercial products are referenced in the text, this does not imply endorsement but is included for completeness.

the live-time clock has a frequency of 10 kHz and a pulse width of 10 ns. The relative standard uncertainty of this frequency is lower than 10^{-9}.

3.3 Measurements:

Each measurement set was presented in the files described in 3.4 as: raw data for the blank, raw data for the source and net data (i.e. blank corrected). These measurements were the result of 10 repetitions and the counting time (live time) of each repetition was 60 s. The standard deviations of the raw values were the experimental standard deviations of the repetitions and *not* the standard deviations of the means. The standard deviations of the net counting rates were calculated as the quadratic sum of the standard deviation of the blank and the source counting rates. It was indicated in the protocol that if the standard deviation of the mean was to be used in the calculation of the uncertainty, the experimental standard deviations had to be divided by the square root of 10, which corresponds to the number of repetitions. The covariances between the double counting rates and between the double and triple counting rates were the experimental covariances, calculated from the repetition of the data acquisition and it was mentioned that the reported information were experimental covariances and not covariances between the means of the values. Standard deviations of the various TDCR values (i.e. individual doubles divided by triples and logical sum of the doubles divided by triples) could be calculated using the given information and the formulae used were described in the "comments" sheet of the Excel file.

The checksums AB+BC+AC and 2T+S were given to show the consistency of the data. The two checksums presented in the raw acquisition files are AB+BC+AC-2T-D and A+B+C-T-D-S. The values of these two checksums should be equal to zero if all information is coherent.

3.4 Contents of the files:

- **H3_KCWG_2014.xls**, Excel file presenting the main results in two sheets: grey filters, defocusing and a sheet describing the measurements.
- **H3_defocus.txt,** raw acquisition file for PMT defocusing. The first part relates to the measurement of the blank source for various focusing potentials and the second part relates to the tritium source.
- **H3_filters.txt,** raw acquisition file for blank and tritium sources, with and without three grey filters with various optical densities.

4 Time schedule

The distribution of the experimental data set to the participants was made in October 2015, after approval of the comparison protocol by the Key Comparison Working Group (KCWG) of the Consultative Committee on Ionizing Radiation, Section II (CCRI(II)). The initial deadline for reporting the results was initially fixed at 31 January 2016, then was postponed to 29 February 2016, at the request of two participants. It was mentioned in the protocol that no results should be sent to LNE-LNHB before the announcement that LNE-LNHB had submitted its results to the Bureau International des Poids et Mesures (BIPM). Its submission was made on 11 February 2016 and the participants were then informed that they could send their results to LNE-LNHB. The preliminary results of this comparison were presented in an anonymous way at the KCWG CCRI(II) meeting at the BIPM on 17-18 March, 2016.

5 Calculation methods

The calculation methods used by the participant laboratories are detailed hereafter and summarized in Table 2.

5.1 ANSTO

To calculate the detection efficiency, ANSTO used the TDCR07c code [2], from LNE-LNHB, with minor modifications. The main modification concerns the calculation of the stopping power: the data from Tan & Xia (2012) [3] is used from 20 eV to 10 keV and a linear extrapolation to zero is used under 20 eV. The Bethe formula (ICRU 37, [4]) is used over 10 keV. The cocktail density is varied between 0.960 and 0.993, the *Z/A* ratio is varied between 0.545 and 0.549, the mean excitation energy is varied between 0.062 and 0.065 keV and the *kB* value is varied between 0.007 and 0.015 cm/MeV, with a uniform distribution. Covariance between counting channels are considered.

5.2 CENTIS

To calculate detection efficiency, the CENTIS used the TDCR07c-CENTIS code, which is a variant of the original TDCR07c code. The main modifications concern the use of a Polya statistics instead of a Poisson statistics and the stopping power values of Tan & Xia [3] under 100 eV instead of a linear extrapolation to zero.

5.3 CNEA

CNEA used the TDCR07c code to calculate the detection efficiency and the uncertainties were calculated using an Excel spreadsheet. The influence of the *kB* factor was evaluated by considering a uniform distribution.

5.4 ENEA

The TDCR07c code was used by ENEA to calculate detection efficiency. The *kB* values considered were in the 0.007 to 0.015 cm/MeV range, with an optimal value of 0.010 cm/MeV obtained by minimizing the slope of the relation between the activity and the TDCR value.

5.5 FTMC

The code used by FTMC to calculate detection efficiency is TDCR2014, described as an updated version of TDCR07c. Covariance terms were not taken into account in the uncertainty evaluation.

5.6 IFIN-HH

The TDCR07c code was used at IFIN-HH to calculate the detection efficiency. The density of the cocktail was 0.98 g/cm^3, the mean excitation energy 50 eV, the lower integration bound of the Birks formula 60 eV and the *kB* value was varied between 0.007 and 0.015 cm/MeV with a uniform distribution, and the optimum value was determined as 0.010 cm/MeV, by minimization of the slope of the relation between the activity and the TDCR value. The covariances between the experimental counting rates were taken into account.

5.7 IRA-METAS

A locally-developed code was used at IRA-METAS. The beta spectrum was calculated by including a shape factor function from Wilkinson [5], a weak electron screening approximation from Behrens and Büring [6], an electron exchange model from Harson and Pyper [7] and some further corrections (finite size, recoil, radiative) from Wilkinson [5]. A final state correction was also included to account for the possibility for some decays to result in excited atomic states [8]. The stopping power function is from ESTAR (NIST) [9] over 100 eV and is linearly extrapolated to zero below 100 eV. For the assessment of uncertainties, four additional functions were used: three were calculated from Gümüs [10] and Tan & Xia [3], with additional radiative stopping power from ESTAR and the last one using the function given by Grau Carles and Grau Malonda [11]. The mean excitation energy of the cocktail was taken to be 64.87 eV, based on the elemental composition given by Rodriguez Barquero and Los Arcos [12] and the ICRU 37 report [4]. The lower integration bound of the Birks formula was taken as zero and the *kB* value was explored in the 0.0075 to 0.012 cm/MeV range, using a rectangular distribution and leading to an optimum value of 0.0098 cm/MeV with a standard deviation of 0.0013 cm/MeV, by minimization of the slope of the activity versus efficiency curve. The asymmetry was taken into account. The uncertainties were evaluated using the GUM supplement 1 approach, taking into account the covariances.

5.8 EC-JRC

The code TDCRB-02p [13] was used at EC-JRC to calculate the detection efficiency. The stopping power was calculated with the Birks formula over 100 eV and extrapolated linearly to zero under this energy. The density of the cocktail was taken as 0.985 g/mL and the mean excitation energy as 65.12 eV. The lower integration bound of the Birks formula was taken as zero. The *kB* parameter was considered as a Gaussian random number with a mean value of 0.0112 cm/MeV and a standard deviation of 0.0011 cm/MeV. The asymmetry of the tubes was taken into account. For comparison, four other codes were considered: EFFY5 [14], MICELLE2 [15], TDCRB-02p with Polya distribution and TDCR07c but these results were not taken into account in the final result.

5.9 KRISS

The code used at KRISS to calculate the detection efficiency was EFFICAL from LNE-LNHB. The stopping power is calculated using the ICRU 37 formula [4]. The density of the cocktail was taken as 0.98 g/cm^3 and the mean excitation energy as 64.57 eV. The lower integration bound of the Birks formula was taken as 60 eV and the *kB* value was considered as a uniform random variable with a mean value of 0.006 cm/MeV and a standard deviation of 0.002 cm/MeV. The asymmetry of the photomultiplier tubes was not considered and the optimum *kB* value was obtained by minimizing the slope of the relation between the activity and the TDCR value.

5.10 LNE-LNHB

The TDCR07c code was used at LNE-LNHB together with a locally developed Monte Carlo engine, the MOULINETTE code. The density of the cocktail was taken as 0.98 g/cm^3 and the mean excitation energy was calculated as 64.6 eV, which is also the value chosen as the lower integration bound of the Birks formula. The *kB* parameter was considered as a uniform random variable with a mean value of 0.010 cm/MeV and a standard deviation of 0.006 cm/MeV. The uncertainties were calculated using the GUM supplement 1 method, the experimental counting rates being selected by a Bootstrap technique, taking into account the

correlation between the coincidence channels.

5.11 NIM

The TDCR07c code was used at NIM to calculate the detection efficiency. The stopping power function used was the ICRU 37 formula [4] over 100 eV and a linear extrapolation to zero under this value. The density of the cocktail was 0.978 g/cm^3 and the mean excitation energy 64.6 eV, which was also used as the lower integration bound of the Birks formula. The *kB* parameter was varied in the 0.010 to 0.013 cm/MeV range with an optimum value chosen by the least-square minimization of the slope of the relation between activity and TDCR value.

5.12 NIST

The TDCR calculations were carried out at NIST by use of purpose-built program written in Mathematica®. Several versions of the base code were created for evaluation of uncertainties and other auxiliary programs in Matlab® were used for the decorrelation of counting data. The spectrum calculation was carried out by the BETASPEC [16] program from LNE-LNHB, which is the beta spectrum calculation program embedded in the TDCR07c code. The stopping power was calculated by fitting the ESTAR [9] data given the cocktail composition found in MICELLE2 code [15]. The density of the cocktail was 0.985 g/cm^3 and the lower integration bound of the Birks formula was taken as 1 eV. The *kB* parameter was considered as a Gaussian random variable with a mean value of 0.0075 cm/MeV and a standard deviation of 0.0010 cm/MeV. The asymmetry of the photomultiplier tubes was taken into account, by using the [Solve] function (which is an implementation of Newton's method) to solve the three TDCR equations. The optimum *kB* value was chosen by minimization of the variance relationship of activity versus efficiency, combined with previous experience with this cocktail and this radionuclide. The uncertainty was evaluated using the GUM supplement 1 method.

5.13 NPL

The TDCR calculation was carried out using a NPL in-house written FORTRAN library called from Excel. The beta spectrum was calculated with the Fermi function including effects of finite nuclear size, validated by comparisons with Behrens, Jänecke and Landolt-Börnstein tables [18]. The screening correction was taken from Rose and Durand [19] and all other corrections were taken from the tabulations of Wilkinson [5]. The stopping power was calculated using a cubic spline interpolation of the ESTAR data [9] with an energy cutoff of 1 keV. Under 1 keV, the curve was linearized with the gradient at the last data point to allow extrapolation at low energy. The density of the cocktail was taken as 0.978 g/cm^3.The lower integration bound of the Birks formula was taken as the energy divided by a factor of 500. The *kB* value was varied from 0.0075 cm/MeV to 0.0120 cm/MeV, assuming a rectangular distribution. The optimal value of 0.0090 cm/MeV was chosen by minimization of the slope of activity versus the efficiency. The asymmetry of the photomultiplier tubes was not taken into account but an uncertainty contribution was added in the uncertainty budget.

5.14 NRC

The codes MICELLE2 [15] and TDCR07c [2] were used at NRC to calculate detection efficiency but only the results obtained by the former code were selected as a final result. NRC reported that the calculated beta spectra obtained with the two codes were inconsistent. The electron stopping power formula was from Rohrlich and Carlson (ICRU 37 [4]) above 1

keV and an empirical formula was used under this value. The density of the cocktail was taken as 0.98 g/cm^3 and the mean excitation energy as 47 eV. The *kB* factor was considered in a 0.005 to 0.015 cm/MeV range and the optimum value of 0.0085 cm/MeV was obtained by minimization of the slope of the relation between the activity and the TDCR value. The asymmetry of the photomultiplier tubes was not taken into account in the calculation of the detection efficiency but its influence was studied by the TDCR07c code and a corresponding uncertainty contribution was added to the final result.

5.15 POLATOM

The locally developed code TDCRB-03 code, based on the TDCRB-1 code [13], was used by POLATOM to calculate detection efficiency. The beta spectrum was calculated using SPEBETA. The stopping power was calculated using the Bethe-Bloch formula over 100 eV and extrapolated linearly under 100 eV. The density of the cocktail was taken as 0.985 g/cm^3, the mean excitation energy as 62.46 keV and the lower integration bound of the Birks formula was zero. The *kB* factor was considered in a (0.0092 ± 0.0004) cm/MeV range and the optimal value selected by minimizing the relation between the activity and the TDCR value. The asymmetry of the photomultiplier tubes was taken into account and the uncertainties were evaluated within the GUM framework.

5.16 PTB

A specific PTB code using modified routines from EFFY4 [14] and KB [20] codes was used at PTB to calculate the detection efficiency. The stopping power formula was the one used in the KB code, the density of the cocktail was taken as 0.982 g/cm^3, the mean excitation energy of the cocktail was 65 eV and the lower integration bound of the Birks formula was taken as zero. The *kB* value was considered as a Gaussian random variable with a mean value of 0.0075 cm/MeV and a standard deviation of 0.0010 cm/MeV, with an optimum value selected by the minimization of the slope of the relation between the activity and the detection efficiency, taking also into account previous tritium measurement at PTB when using chemical quenching to vary the efficiency. The asymmetry of the photomultiplier tubes was considered and the uncertainty was evaluated in the framework of the GUM.

5.17 VNIIM

The TDCR07c code with its standard options was used at VNIIM to calculate the detection efficiency. The *kB* value was considered in the 0.009 to 0.011 cm/MeV range and the optimum value was selected by minimizing the slope of the activity versus efficiency curves. The uncertainty was evaluated in the framework of the GUM.

6 Uncertainty budget

The uncertainty budgets reported by the participants are presented in Table 3. The dominant uncertainty contribution generally comes from the *kB* factor but several laboratories reported a non-negligible contribution from the model (Poisson or Polya statistics) and also from the lower integration bound of the Birks formula. In general, as it can be observed in Figure 1, there is a large dispersion (factor of 4) of the reported combined uncertainties. This dispersion can be explained by the range and the probability density function (*pdf)* of the considered *kB* values. Some laboratories considered a 0.007 to 0.015 cm/MeV range with a uniform *pdf* and others restricted this range on the basis of the slope observed between the activity and the detection efficiency. This makes a difference because, if the *pdf* of the *kB* is supposed to be

uniform, the standard deviation is the difference between the interval bounds divided by the square root of 12, i.e. about 3.5, but if this *pdf* is supposed to be Gaussian, the corresponding standard deviation is approximately the difference between the interval bounds divided by 6 (plus and minus three standard deviations). Thus, the uniform assumption leads to a significantly larger uncertainty.

Figure 1 Distribution of combined standard uncertainties reported by the participants

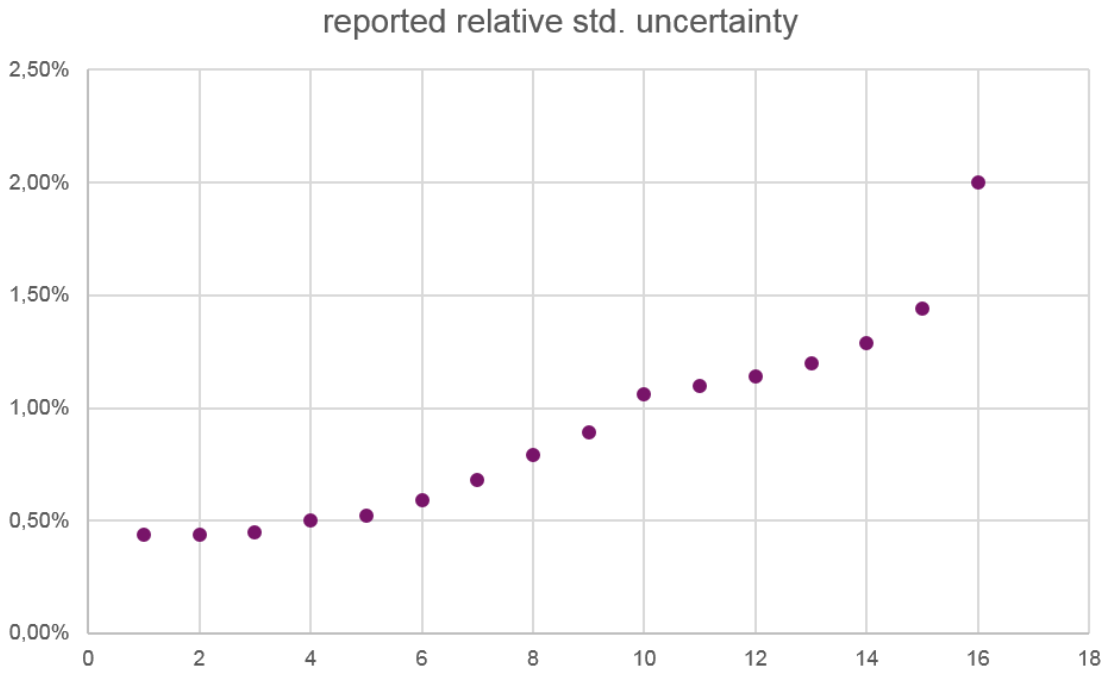

Table 2: Calculation methods, codes and parameters reported by the participants

Laboratory	Calculation code	*kB* range in cm/MeV	*kB pdf*	Optimum *kB* value in cm/MeV	*dE/dx* calculation model	Quenching formula	Lower integration bound	Asymmetry considered	Spectrum model	Uncertainty calculation	Covariances considered
KRISS	EFFICAL	0.006-(2)	slope uniform	0.006(2)	ICRU37	Birks	60eV	no	SPEBETA	GUM	no
NPL	local	0.075-0.012	slope uniform	0.009	ESTAR	Birks	35eV	no	Rose	GUM	yes
POLATOM	TDCRB-03	0.0092(4)	slope	0.0092	ICRU37+lin extrapolation	Birks	0	yes	SPEBETA	GUM	no
ENEA	TDCR07c	0.007-0.015	slope	0.01	ICRU37+lin extrapolation	Birks	64 eV	yes	SPEBETA	GUM	yes
VNIIM	TDCR07c	0.009-0.011	slope	0.010(1)	ICRU37+lin extrapolation	Birks	0	yes	SPEBETA	GUM	no
NIM	TDCR07c	0.010-0.013	slope		ICRU37+lin extrapolation	Birks	60eV	yes	SPEBETA	GUM	no
IFIN-HH	TDCR07c	0.007-0.015	slope	0.01	ICRU37+lin extrapolation	Birks	60eV	yes	SPEBETA	GUM	yes
NIST	local	0.0075-0.0085	Slope uniform	0.0075(10)	ESTAR	Birks	1 eV	yes	BETASPEC	GUM. GUM1	yes
EC-JRC	TDCRB-02	0.0112(11)	slope		ICRU37+lin extrapolation	Birks	0	yes	SPEBETA	GUM	no
LNE-LNHB	MOULINETTE	0.009-0.011	slope uniform	0.01	ICRU37+lin extrapolation	Birks	64.6	yes	SPEBETA	GUM. GUM1	yes
FTMC	TDCR2014	0.007-0.015	slope	0.01	ICRU37+lin extrapolation	Birks	64.2	yes	SPEBETA	GUM	no
CENTIS	TDCR07c mod	0.009-0.011	slope uniform	0.010(1)	Tan Xia < 10keV	Birks	65eV	yes	SPEBETA	GUM	yes
CNEA	TDCR07c	0.007-0.015	slope uniform	0.011	ICRU37+lin extrapolation	Birks	60eV	yes	SPEBETA	GUM	no
ANSTO	TDCR07c	0.007-0.015	slope. uniform	0.011(2)	Tan Xia < 10keV	Birks	0-63 eV	yes	Rose	GUM	yes
IRA-METAS	local	0.0075-0.012	slope uniform	0.0098(13)	various	Birks	0	yes	detailed	GUM1	yes
PTB	local	0.0075(10)	slope	0.0075(10)	kB code	Birks	0	yes	EFFY4	GUM	no
NRC	MICELLE2	0.005-0.015	slope	0.0085	Bethe+lin extrap	Birks	1eV	no	Included in MICELLE2	GUM. GUM1	yes

Table 3 Uncertainty budgets reported by the participants

	ANSTO		CENTIS	
Input quantity	**Relative standard uncertainty %**	**Comments**	**Relative standard uncertainty %**	**Comments**
Counting rates	0.054	std deviation of the weighted mean	0.09	
Dead time			0.01	uniform pdf
Blank		included in counting rates	0.0007	
Pile-up			0.1	uniform pdf
Counting time	0.03	Live-time uncertainty	0.05	
Model and input parameters	0.22	Poisson vs.Polya	1	uniform pdf
kB	0.66	0.011 (2) cm/MeV. uniform pdf	0.4	uniform pdf
dE/dx	0.12	Tan and Xia vs. Bethe		
Integration bound	0.52			
Scintillator composition	0.12	Density. *Z/A* and mean excitation energy		
Spectrum	0.007	18.564 (3) keV. normal pdf		
Accidental coincidences	0.045	Counting statistics and resolving time		
Decay	0.0013	Uncertainty in decay time		
Impurities			0.1	
Combined	0.89		1.1	

Table 3, continued

	CNEA		FTMC		ENEA	
Input quantity	**Relative standard uncertainty %**	**Comments**	**Relative standard uncertainty %**	**Comments**	**Relative standard uncertainty %**	**Comments**
Counting rates	0.077		0.13		0.25	
Dead time			0.05		0.08	
Blank			0.08			
Pile-up			0.06			
Counting time						
Model and input parameters			0.01		0.6	
kB	0.34	uniform pdf	0.49			Included in model input parameters
dE/dx						Included in model input parameters
Integration bound						
Scintillator composition						
Spectrum						
Accidental coincidences						
Decay						
Combined	0.5		0.52		0.65	For filters

Table 3, continued

	IFIN-HH		LNE-LNHB	
Input quantity	**Relative standard uncertainty %**	**Comments**	**Relative standard uncertainty %**	**Comments**
Counting rates	0.103		0.52	Bootstrap Monte Carlo
Dead time	0.006		0.01	
Blank	0.0037			included in counting rates
Pile-up	0.0253	considering counting rate and coincidence resolving time	0.01	
Counting time	0		0.1	
Model and input parameters	0.34	Poisson and Polya statistics	0.01	
kB	0.676	uniform pdf		included in Monte Carlo calculation (uniform pdf)
dE/dx				
Integration bound				
Scintillator composition				
Spectrum	0.0054	maximum beta energy	0.005	Gaussian pdf
Accidental coincidences				
Decay				
Combined	0.684	grey filters. but similar values for defocusing	0.53	

Table 3, continued

	IRA-METAS		EC-JRC	
Input quantity	**Relative standard uncertainty %**	**Comments**	**Relative standard uncertainty %**	**Comments**
Counting rates	0.13	correlated Gaussian samples or T and 3 D	0.07	
Dead time	0.01	uncertainty of live-time clock	0.06	
Blank	0.02	correlated Gaussian samples or T and 3 D	0.008	
Pile-up				
Counting time			0.004	
Model and input parameters			0.3	
kB	1.2	uniform pdf	0.6	
dE/dx				
Integration bound				
Scintillator composition				
Spectrum	0.003	maximum beta energy		
Accidental coincidences				
Decay	0.001			
deviation of measurements	0.78	std deviation of the mean of grey filters and defocusing		
PMT asymmetry			0.05	
Combined	1.44		0.68	

Table 3, continued

	KRISS		NIM		VNIIM	
Input quantity	**Relative standard uncertainty**	**Comments**	**Relative standard uncertainty**	**Comments**	**Relative standard uncertainty**	**Comments**
Counting rates	0.04		0.17		0.06	
Dead time	0.56		0.01			
Blank			0.04		0.0016	
Pile-up						
Counting time			0.01			
Model and input parameters						
kB	1.16		0.4	uniform pdf	0.45	
dE/dx						
Integration bound						
Scintillator composition						
Spectrum						
Accidental coincidences						
Decay						
TDCR repeatability	0.04					
Combined	1.29		0.44		0.45	

Table 3, continued

	NIST		NPL	
Input quantity	**Relative standard uncertainty**	**Comments**	**Relative standard uncertainty**	**Comments**
repeatability	0.24	experimental std deviation	0.34	normal pdf
Counting rates	0.2	Poisson pdf	0.072	
Dead time	2.00E-04		1.50E-01	normal pdf
Blank	0.07	Bootstrap Monte Carlo	0.02	
Pile-up			0.02	normal pdf
Counting time			< 0.001	
Model and input parameters	0.11		0.33	normal pdf
kB	0.94	uniform pdf	0.75	rectangular pdf
dE/dx				
Integration bound	0.05			
Efficiency calculation	0.34	Bootstrap Monte Carlo		
Scintillator composition			0.05	normal pdf
Spectrum	0.11	uniform pdf	0.037	normal pdf
Accidental coincidences				
Decay	9.00E-05		< 0.001	normal pdf
Adsorption effects			5.00E-03	normal pdf
PMT asymmetry			7.30E-01	normal pdf
Impurities			1.00E-02	assumed none present
Electron exchange effect			1.00E-01	normal pdf
Combined	1.06		1.2	

Table 3, continued

	NRC		POLATOM		PTB	
Input quantity	**Relative standard uncertainty**	**Comments**	**Relative standard uncertainty**	**Comments**	**Relative standard uncertainty**	**Comments**
Counting rates	0.1		0.2		0.14	
Dead time	<< 0.01				0.03	from experience at PTB
Blank		included in counting rates	0.01		0.02	
Pile-up					n.a.	
Counting time			0.004		0.01	
Model and input parameters	2	normal pdf	1.1		0.3	including asymmetry
kB	0.3	normal pdf	0.26		0.7	Included in *kB* uncertainty component
dE/dx						included in kB
Integration bound						
Scintillator composition						
Spectrum					0.1	
Accidental coincidences						
Decay	0.001	normal pdf			negligible	
PMT asymmetry	0.1	normal pdf				Included in “model and input parameters”
models: Larkins and Micelles	0.03	normal pdf				
Experimental TDCR					0.07	
Combined	2		1.14		0.79	

7 Final results

The final results are presented in Table 4 and graphically in Figure 2. The characteristics of the distribution of the results, evaluated using the PomPlot software [22], are reported in Table 5. It can be observed that all the results are compatible, within the reported uncertainties, and that the values of the arithmetic mean, the weighed mean, the power-moderated mean and the median are very similar.

Table 4 Final results reported by the participants

Number	NMI/DI	Activity in kBq	Standard uncertainty in kBq	Relative standard uncertainty
1	KRISS	11.24	0.15	1.3%
2	NPL	11.32	0.13	1.1%
3	POLATOM	11.44	0.13	1.1%
4	ENEA	11.468	0.05	0.44%
5	VNIIM	11.468	0.05	0.44%
6	NIM	11.47	0.05	0.44%
7	IFIN-HH	11.471	0.07	0.61%
8	NIST	11.49	0.12	1.0%
9	EC-JRC	11.515	0.08	0.69%
10	LNE-LNHB	11.53	0.06	0.52%
11	FTMC	11.54	0.06	0.52%
12	CENTIS	11.54	0.13	1.1%
13	CNEA	11.54	0.06	0.52%
14	ANSTO	11.56	0.11	0.89%
15	IRA-METAS	11.57	0.17	1.5%
16	PTB	11.57	0.10	0.86%
17	NRC*	11.716	0.23	2.0%

- NRC also reported the value obtained using the TDCR07c code: 11.45 (24) kBq but this value is not used as their declared comparison value.

Table 5 Statistical characteristics of the results

Quantity	Value, kBq	Standard uncertainty, kBq
Arithmetic mean	11.497	0.025
Weighted mean	11.495	0.018
Median	11.515	0.022
Weighted median	11.471	0.015
Power-moderated mean with $\alpha=2$	11.495	0.019

Figure 2. Final results

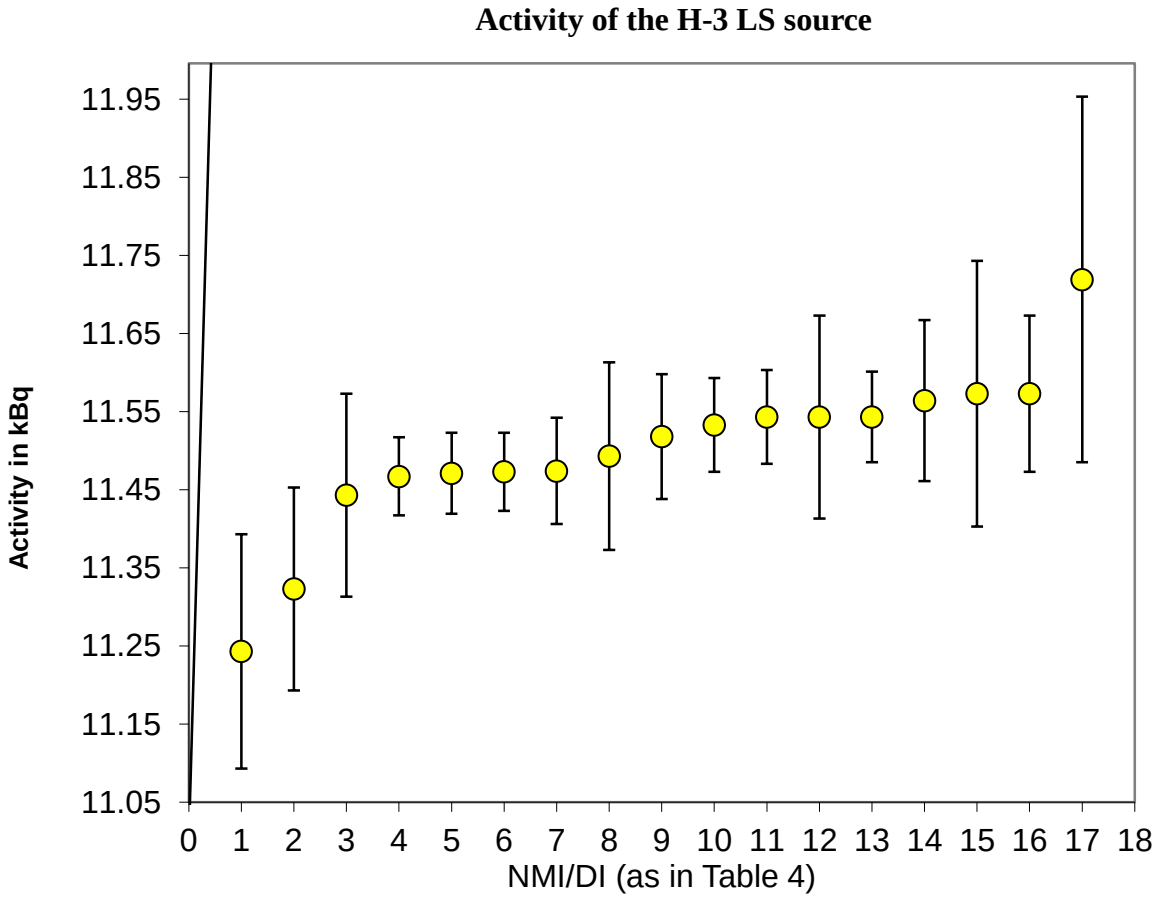

8 Analysis of the factors of influence

Some factors of influence were analysed to explain the variability of the results. This includes the effect of asymmetry, the software used, the *kB* value and stopping power formula and the tritium spectrum. These influences are reported hereafter.

8.1 Asymmetry

The consideration of the asymmetry of the photomultiplier tubes is an obvious factor of influence in the results, as it can be observed in Figure 3. The relative experimental standard deviation of all the results is about 0.9 % and this value is reduced to 0.4 % when considering only the results obtained by considering the asymmetry.

Figure 3. Influence of considering the asymmetry in the calculation model

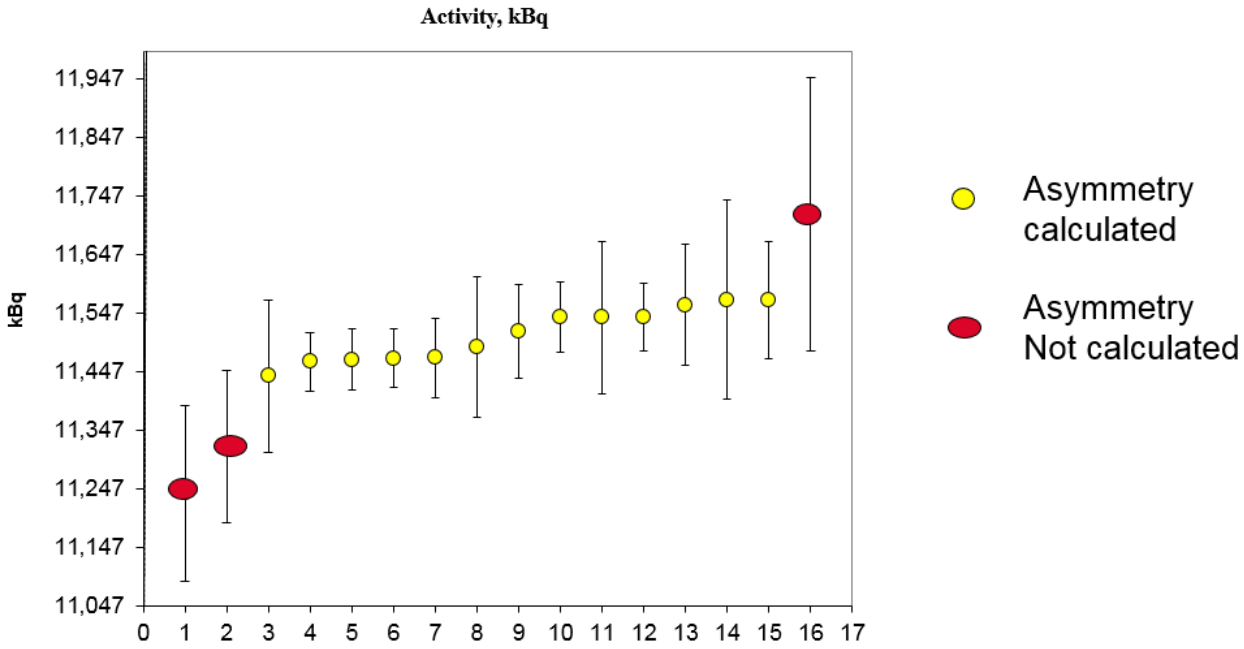

8.2 Influence of the software used to calculate detection efficiency

As expected, the results obtained by the nine laboratories using the TDCR07c code are quite similar in their mean value, but it can be observed in Figure 4 that this is not the case for the reported uncertainties. Nevertheless, it must be pointed out that the four laboratories which used other software packages reported results very close to the ones obtained using TDCR07c and thus that the variability in the results cannot be only attributed to the calculation code used. This also shows that there is a "user effect", because one could expect that the same dataset treated by the same code would produce the same results, which is not the case. Two more comments can be added: first, the use of the same code by many laboratories obviously introduces a correlation between the results, even if there is a "user effect"; second, most of the TDCR codes used in this exercise are based on the same physical models (statistics, Birks model, etc.) and thus, this correlation exists between all the results. The best way to avoid such correlation is to use different physical models based on different principles.

Figure 4. Influence of the calculation code

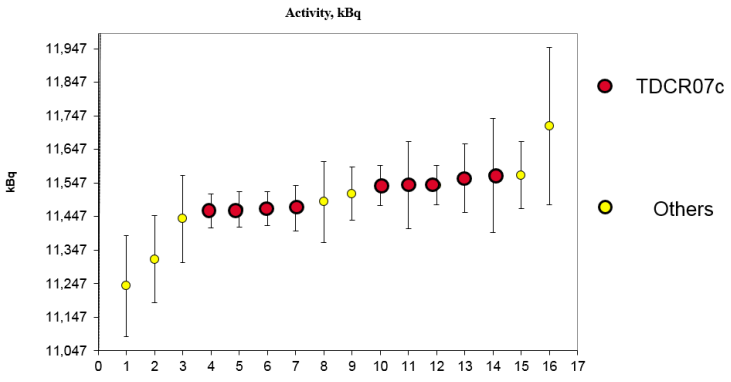

8.3 *kB* factor and stopping power formula

All the laboratories obtained the optimal value of the *kB* factor by minimization of the slope between the activity and the detection efficiency, or the TDCR value. As for tritium, the relation between the TDCR and the efficiency is almost linear, it can be considered that both approaches are similar. It is well known that comparison of *kB* factors used in the TDCR method is not relevant, if the formula used to calculate the electron stopping power function is not taken into account, as these two elements are multiplied in the Birks formula. It can be observed in Figure 5 that there is no obvious correlation between the *kB* value used and the activity reported for most of the results. For the lowest *kB* value reported, the associated stopping power function used was the ICRU37 formula [3], but no details are given on how this formula was managed at low energy. This is perhaps the explanation of the low activity value reported, but, this could also be the consequence of not considering the asymmetry of the photomultiplier tubes in the calculation.

Figure 5. Influence of the value of the kB factor on the activity as reported by participants

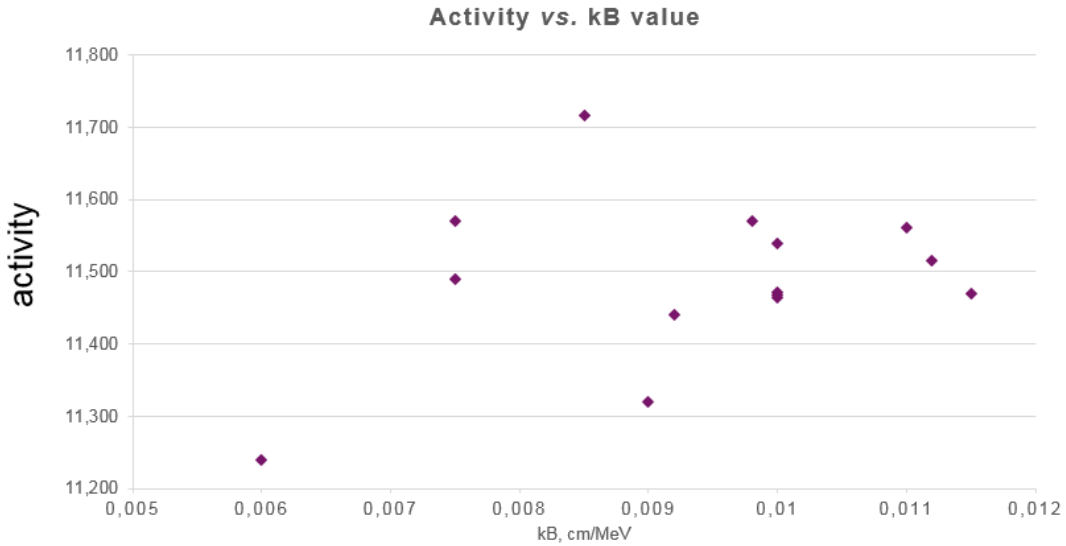

8.4 Tritium calculated spectrum

All the reported ^{3}H beta spectra are similar, the difference between the spectrum obtained using the classical Fermi function, like the one included in the codes EFFY [14] or SPEBETA [16], and the very sophisticated calculation used by IRA-METAS is negligible. As expected, for such low-Z allowed transition, the shape of the beta spectrum is not likely to be an important influence.

8.5 Comparison with the results obtained during the CCRI(II) K2-H3 activity comparison

In this exercise, all the activity results reported by the participants were calculated from the same dataset. It is interesting to compare this to the results obtained during the H-3 K2 CCRI(II) comparison in 2009 [23], in order to separate the variability causes due to the experimental devices and those due to the calculations. The results, scaled for comparison to

get a similar mean activity to that in the present exercise, can be observed in Figure 6, but, as the participants in the two exercises were different, the number on the x axis does not correspond to the same NMI/DI in Figure 2 and Figure 6. The dispersion is much higher in the case of the K2 comparison, with a Birge ratio of 1.96 compared to the Birge ratio of 0.79 obtained in the present exercise. This can also be confirmed by the comparisons of the PomPlot's [21] of the two exercises shown in Figure 7. This highlights the influence of the counter and its adjustment for the measurement of tritium. It must be observed that the measurands are not identical in the two exercises, (the K2 exercise was about an activity per unit mass), but it can be assumed that the weighing process is not the dominant source of variability in such measurement, and thus the comparison between the two exercises makes sense.

Figure 6. Results of the K2 H-3 CCRI(II) comparison. The values were scaled to make comparison with Figure 2 easier.

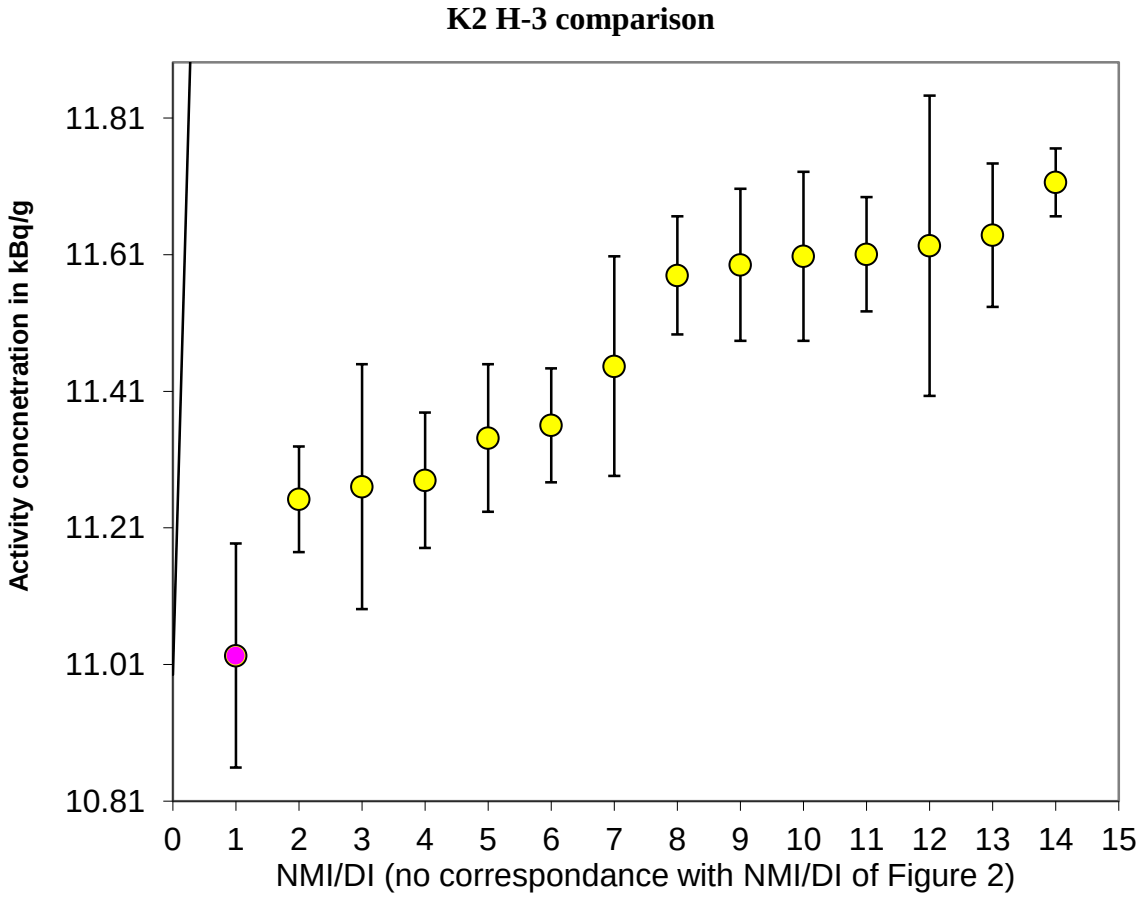

Figure 7. PomPlot's of the S12 and K2 H-3 CCRI(II) comparisons

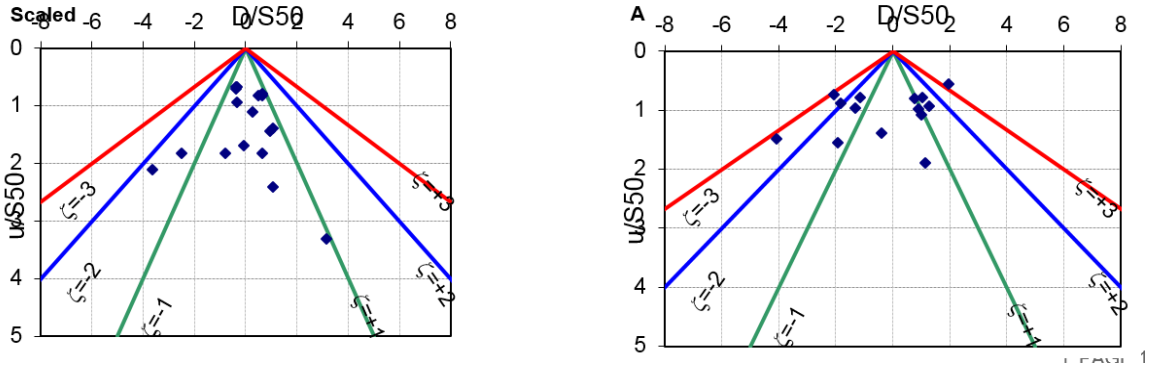

Conclusions

This CCRI(II) S-12 H-3 exercise gave the opportunity to test and compare the calculation methods used to measure the activity of a liquid scintillation source in the framework of the TDCR model. This comparison involved quite a large number of participants (17) and all the reported results are compatible within the uncertainties. The estimators of the distribution of the results are very robust, and indicate that these results can be considered as normally distributed. Even if the good consistency of the results is positive for the international traceability of radionuclides by TDCR measurements, it must be observed that the uncertainty evaluation is still far from being homogeneous in the National Metrology Institutes and also that a large number of the results are correlated by the use of the same calculation code and of the same physical models. Nevertheless, these physical models can be considered as the current state of the art but we hope that different approaches to the model of the ionization quenching will be developed in the future, leading to more robust calculations. This could be achieved by using experimental non-linearity relations obtained with Compton spectrometers, but also by developing a more sophisticated Monte Carlo description of the energy transfer phenomena occurring inside a liquid scintillator. These new approaches are currently under development in several laboratories.

Acknowledgements

The participants acknowledge John Keightley, NPL, chairman of the KCWG of CCRI(II) and José Maria Los Arcos, BIPM, for their help in the organization of this comparison.

References

[1] J. Bouchard and P. Cassette, 2000. MAC3: an electronic module for the processing of pulses delivered by a three photomultiplier liquid scintillation counting system. *Appl Radiat Isot.* 52(3).

[2] TDCR07c code. http://www.nucleide.org/ICRM_LSCWG/icrmsoftware.htm

[3] Z. Tan and Y. Xia, 2012. Stopping power and mean free path for low-energy electrons in ten scintillators over energy range 20 – 20 000 eV. *Appl Radiat Isot.* 70.

[4] ICRU, 1984. Stopping powers for electrons and positrons, ICRU report. International Commission on Radiation Units and Measurements, Bethesda, MD, USA, vol 37.

[5] D. H. Wilkinson, 1989. Evaluation of Beta Decay I. The Traditional Phase Space Factors, *Nuclear Instruments and Methods* **A275**. D. H. Wilkinson, 1991. Small terms in the beta decay spectrum of tritium, *Nuclear Physics* ***A526***. D. H. Wilkinson, 1990. Evaluation of Beta Decay II. Finite mass and size effects, *Nuclear Instruments and Methods* ***A290***. D. H. Wilkinson, 1993. Methodology for Superallowed Fermi Beta-Decay Part II. Reduction of Data, *Nuclear Instruments and Methods* ***A335***.

[6] H. Behrens and W. Bühring, 1982. Electron radial wave functions and nuclear beta-decay. Clarendon Press, Oxford.

[7] M. R. Harston and N. C. Pyper, 1993. Atomic effects on the *ft* value for tritium β decay, *Phys. Rev.* ***A 48***.

[8] A. Saenz, S. Jonsell, and P. Froelich, 2000. Improved Molecular Final-State Distribution of HeT+ for the β-Decay Process of T2, *Phys. Rev. Lett.* ***84***.

[9] M. J. Berger, 1993. ESTAR, PSTAR AND ASTAR, a PC package for calculating stopping powers and ranges of electrons, protons and helium ions, IAEA-NDS-144.

[10] H. Gümüş and Ö. Kabadayi, 2010. Practical calculations of stopping powers for intermediate energy electrons in some elemental solids, *Vacuum* ***85*** and private communication.

[11] A. Grau Malonda and A. Grau Carles, 1999. The ionization quench factor in liquid-scintillation counting standardizations, *Appl. Radiat. Isot.* ***51***.

[12] L. Rodríguez-Barquero, and J. M. Los Arcos, 2010. Experimental determination of elemental compositions and densities of several common liquid scintillators, *Appl Radiat Isot.*

[13] R. Broda, P. Cassette, K. Maletka, K. Pochwalski, 2000. A simple computing program for application of the TDCR method to standardization of pure-beta emitters. *Appl Radiat Isot.* 52 (3).

[14] E. Garcia-Toraño and A. Grau Malonda, 1985. EFFY, a new program to compute the counting efficiency of beta particles in liquid scintillators. *Comput. Phys. Comm.* 36.

[15] K. Kossert and A. Grau Carles, 2010. Improved method for the calculation of the counting efficiency of electron-capture nuclides in liquid scintillation samples, *Appl Radiat Isot.*, Volume 68, Issues 7–8.

[16] P. Cassette, 1992. SPEBETA, programme de calcul du spectre en énergie des électrons émis par des radionucléides émetteurs bêta. Note technique LPRI/92/307/Juillet.

[17] http://materials.springer.com/bp/docs/978-3-540-36068-1

[18] M. E. Rose, 1936. Phys Rev Lett 49 and L. Durand, 1964. Phys Rev 135.

[19] J. M. Los Arcos and F. Ortiz, 1997. KB: a code to determine the ionization quenching function Q(E) as a function of the kB parameter *Comput. Phys. Commun.* 103.

[20] Y. Spasova, S. Pommé and U. Wätjen, 2007. Visualisation of interlaboratory comparison results in PomPlots. *Accred Qual Assur* 12.

[21] G. Ratel, 2011. International comparison of activity measurements of a solution of tritiated water. CCRI(II) meeting, 21-23 June 2011. Unpublished.